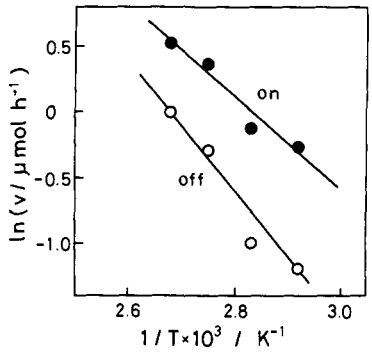

Figure 4. Temperature dependence of C_2H_5OH oxidation: ○, SAW-off; ●, SAW-on.

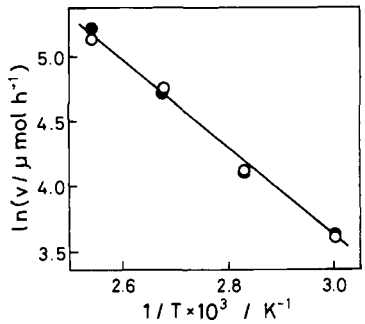

Figure 5. Temperature dependence of C_2H_4 hydrogenation: ○, SAW-off; ●, SAW-on.

its bandwidth was 1.5 MHz at an attenuation of 10 dB. The center frequency was consistent with the value expected from the space between the finger electrodes.

Figure 2 shows the results on the catalytic hydrogenation of ethylene at 333 K. The relationship between the production of ethane and reaction time shows a slightly downward curve because of a gradual decrease in the catalytic activity as the reaction proceeds. Nevertheless, it is obvious that there were no significant changes in ethane production when the SAW was turned on and off. In the reaction of C_2H_5OH with O_2 at 353 K, acetaldehyde is mainly produced. Figure 3 shows that when the SAW was turned on (SAW-on), an immediate increase in the production of acetaldehyde took place; the activity became ca. 2.6 times larger than that in the absence of the SAW (SAW-off). With SAW-off, the activity decreased nearly to the original level before SAW-on. The SAW propagation at rf power will apparently result in the generation of heat on the catalyst, and one might argue about a temperature rise at the catalyst surface. In fact, the temperature of the SAW catalyst measured increased to 363 K immediately after the SAW application. As shown in Figure 3, however, the temperature sharply decreased as a consequence of control by the surrounding electric furnace. After fluctuations, the original level of the temperature was recovered within less than 20 min, whereas the production of acetaldehyde with a higher rate continued over a period of longer than 2 h until the SAW was turned off.

Figure 4 shows the temperature dependence of the oxidation of C_2H_5OH. Without the SAW, the activation energy was evaluated to be 42 kJ mol^{-1}, whereas it decreased to 29 kJ mol^{-1} under the conditions of SAW-on. The distinct differences in the activation energy demonstrate that the SAW is able to give a noteworthy influence to the kinetic behavior of the reaction. As shown in Figure 5, on the other hand, there was no significant change in the activation energy for the hydrogenation of C_2H_4 between SAW-on and SAW-off. It is to be noted that the hydrogenation exhibits no activity increases by the SAW, irrespective of its positive activation energy of 27 kJ mol^{-1}. The comparison of temperature dependence in the two reactions indicates that the presence or absence of a SAW effect is dependent upon the kinds of catalytic reactions. From the above-mentioned findings, it is rational to conclude that the activity enhancements are not due to a thermal effect but to one of SAW-inherent phenomena.

In the previous study, poled ferroelectric $LiNbO_3$ having a polarization axis perpendicular to the surface was used as a catalyst support on which the catalytically active phases such as Pd[4] and NiO[5] were deposited, and it was shown that the activation energy of CO oxidation varied according to the direction of the polarization axis. This polarization effect is associated with a static electric field of the underlying ferroelectric surface. The effect of the SAW observed in this study is ascribable to a dynamic behavior; either or both of the displacement of lattice atoms and the fluctuations of an electric field resulting from the surface wave seem to be responsible for the activation of the Pd surface. One of the interesting features is that the SAW is likely to be effective for the reaction involving a polar molecule.

The present study clearly demonstrates that the SAW has a high potential to develop a device-type catalyst whose catalytic activity can be controlled by an external signal. Further study is in progress.

Acknowledgment. This work was supported under a Grant-in-Aid for Scientific Research from the Japanese Ministry of Education, Science and Culture.

(4) Inoue, Y.; Yoshioka, I.; Sato, K. *J. Phys. Chem.* **1984**, *88*, 1148.
(5) Inoue, Y.; Sato, K.; Suzuki, S.; Yoshioka, I. *Proc. Int. Congr. Catal., 8th, 1984*; DECHEMA, Vol. V, Verlag Chemie: Frankfurt am Main, 1984; p 299.

Reaction of In(t-Bu)$_3$ with Dioxygen: Synthesis and Molecular Structure of [(t-Bu)$_2$In(OO-t-Bu)]$_2$

William M. Cleaver and Andrew R. Barron*

Department of Chemistry, Harvard University
Cambridge, Massachusetts 02138
Received July 31, 1989

The autoxidation reactions of group 13 organometallic compounds (MR_3, M = B, Al, Ga, In) are usually uncontrollably fast; lower alkyl derivatives often inflame spontaneously in air, while higher alkyl derivatives, with lower vapor pressures, may char but not ignite. If the supply of oxygen is restricted, a smooth reaction takes place, to yield the alkoxide compounds via alkylperoxo intermediates (eq 1).[1-3] In the case of boron, many of the intermediate peroxides can be isolated, usually as rather unstable oils.[4] Although proposed in a number of studies,[5] no examples of the heavier group 13 analogues of these boron alkyl peroxides have been isolated. We report here the synthesis and structural characterization of the first stable (alkylperoxo)indium compound.

$$\text{M–R} \xrightarrow{O_2} [\text{M–OOR}] \rightarrow \text{M–OR} \qquad (1)$$

The interaction of In(t-Bu)$_3$[6] with an excess (1 atm) of dry oxygen leads to the formation of the alkylperoxo compound (t-Bu)$_2$In(OO-t-Bu) (**1**) (eq 2).[7] Compound **1** may also be prepared, albeit in low yield, by the reaction of In(t-Bu)$_3$ with pyridine

(1) Odom, J. D. *Comprehensive Organometallic Chemistry*; Wilkinson, G., Stone, F. G. A., Abel, E. W., Eds.; Pergamon: Oxford, 1982; Vol. 1, Chapter 4.
(2) Eisch, J. J. *Comprehensive Organometallic Chemistry*; Wilkinson, G., Stone, F. G. A., Abel, E. W., Eds.; Pergamon: Oxford, 1982; Vol. 1, Chapter 6.
(3) Brindley, P. B. *The Chemistry of Peroxides*; Patai, S., Ed.; Wiley: London, 1983; p 807.
(4) (a) Davies, A. G.; Coffee, E. C. J. *J. Chem. Soc. C* **1966**, 1493. (b) Wilke, G.; Heimbach, P. *Justus Liebigs Ann. Chem.* **1962**, *652*, 7.
(5) Davies, A. G. *Organic Peroxides*; Swern, D., Ed.; Wiley: London, 1971; Vol. 2, Chapter 4.
(6) Bradley, D. C.; Frigo, D. M.; Hursthouse, M. B.; Hussain, B. *Organometallics* **1988**, *7*, 1112.
(7) A yellow solution of In(t-Bu)$_3$ (1.00 g, 3.50 mmol) in pentane (50 mL) was cooled to 0 °C. Dry O_2 was bubbled through the solution until the solution became colorless, <1 min. The solvent was removed under vacuum, yielding a white crystalline solid, which can be recrystallized from pentane (−20 °C). Yield: 60–70%. ^{1}H NMR (δ ppm, C_6D_6): 1.49 (s, 18 H, In-t-Bu), 1.15 (s, 9 H, OO-t-Bu).

0002-7863/89/1511-8966$01.50/0

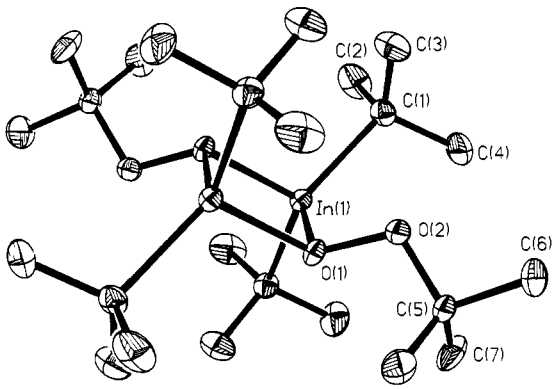

Figure 1. The molecular structure of $[(t\text{-Bu})_2\text{In}(\text{OO-}t\text{-Bu})]_2$. Thermal ellipsoids are shown at the 50% probability level, and hydrogen atoms are omitted for clarity.

N-oxide.[8] Attempts to synthesize **1** by the reaction of $\text{In}(t\text{-Bu})_3$ with *t*-BuOOH have, however, failed.

$$\text{In}(t\text{-Bu})_3 + \text{O}_2 \rightarrow (t\text{-Bu})_2\text{In}(\text{OO-}t\text{-Bu}) \quad (2)$$
$$\mathbf{1}$$

Compound **1** is moisture sensitive, but is stable indefinitely under an oxygen atmosphere. No reaction is observed between **1** and Lewis bases, e.g., pyridine. The IR spectrum of **1** exhibits a moderate absorption at 870 cm^{-1} attributable to the characteristic (O-O) peroxidic stretching vibration.[1]

Alkylperoxo moieties are known to act as monodentate (η^1) (I), bidentate (η^2) (II), and bridging (μ_2) (III) ligands to transition metals.[9] Since the existence of dimers involving bridging alkoxides

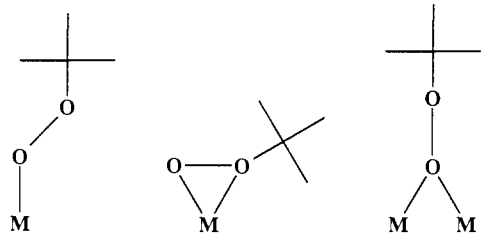

(I) (II) (III)

is a common feature in group 13 chemistry,[10] it would, therefore, be logical to expect the alkylperoxo group in **1** to ligate in a similar fashion. The μ_2-bridging mode of coordination of the *tert*-butyl peroxide group and the dimeric nature of **1** in the solid state have been confirmed by X-ray crystallography.[11]

The molecular structure of **1** is shown in Figure 1. The molecule exhibits overall C_{2h} symmetry with the two indium atoms lying on the 2-fold axis and the alkylperoxo groups on the mirror plane. The In(1)-O(1) distance [2.191 (2) Å] and In(1)-O(1)-In(1a) angle [105.2 (1)°] are similar to those found for other In_2O_2 cores,[6,12] and the In(1)-C(4) bond length [2.199 (4) Å] is in the region previously observed for In-C bonds (2.09-2.25 Å).[11] The peroxo O(1)-O(2) bond distance of 1.484 (4) Å is close to that found for free alkyl hydroperoxides and alkyl peroxides coordinated to transition metals.[9,13] The *tert*-butylperoxo ligand is orientated so as to minimize lone-pair repulsion on the oxygen atoms (IV). A similar *tert*-butyl peroxide geometry was found in the X-ray structural study of the related complex $[(\text{Cl}_3\text{CCO}_2)\text{Pd}(\text{OO-}t\text{-Bu})]_4$.[13]

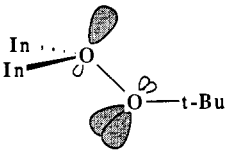

(IV)

The stability of **1** toward further oxidation is unexpected in view of the highly reactive nature of previously reported organoindium compounds toward dioxygen.[14] We propose that this stability is due to the steric hindrance of the *tert*-butyl groups and the strength of the In_2O_2 core, precluding both further attack by O_2 and oxygen transfer from the peroxide to other In-C bonds.

Acknowledgment. Financial support of this work is provided by the donors of the Petroleum Research Fund, administered by the American Chemical Society (Grant No. 20082-G5), the National Science Foundation (Grant No. DMR-86-14003), and ICI Wilton Materials Research Center, U.K. We thank Dr. Joseph W. Ziller and Dr. Simon G. Bott for assistance with the X-ray crystallography.

Supplementary Material Available: Tables of atomic positional and isotropic equivalent thermal parameters, anisotropic thermal parameters, and bond distances and angles for **1** (2 pages); listing of observed and calculated structure factors for **1** (11 pages). Ordering information is given on any current masthead page.

(8) The reaction of $\text{In}(t\text{-Bu})_3$ with pyridine *N*-oxide yields $[(t\text{-Bu})_2\text{In}(\text{O-}t\text{-Bu})]_2$ as the major product, which reacts slowly with excess pyridine *N*-oxide to give small quantities of **1**.

(9) Mimoun, H. *Comprehensive Coordination Chemistry*; Wilkinson, G., Gillard, R. D., McCleverty, J. A., Eds.; Pergamon: Oxford, 1988; Vol. 6, Chapter 1.

(10) Bradley, D. C. *Adv. Chem. Ser.* **1959**, *No. 23*, 10.

(11) Crystal data for $[(t\text{-Bu})_2\text{In}(\text{OO-}t\text{-Bu})]_2$: monoclinic, $C_{2/m}$, a = 16.745 (10) Å, b = 11.453 (9) Å, c = 9.173 (4) Å, β = 117.16 (4)°, V = 1565 (2) Å^3, Z = 8, D(calcd) = 1.350 g cm^{-3}, λ (Mo Kα) = 0.710 73 Å (graphite monochromator), T = -80 °C. A Nicolet R3m/V diffractometer, equipped with an LT-1 low-temperature device, was used to collect 2973 reflections ($4° < 2\theta < 65°$) on a colorless crystal 0.24 × 0.30 × 0.36 mm. Of these, 2865 were independent, and 2540 observed [$F_o > 6\sigma F_o$]. Lorentz and polarization corrections were applied to the data. The In atom was located by direct methods. Standard difference map techniques were used to find the remaining non-hydrogen atoms. All In, O, and C atoms were refined anisotropically. The hydrogen atoms were included as idealized contributions. R = 0.030, R_w = 0.037, final residual = 1.12 e Å^{-3}. All computations used SHELXTL-PLUS: Sheldrick, G. Nicolet XRD, Madison, WI, 1987.

(12) Cleaver, W. M.; Ziller, J. W.; Barron, A. R., unpublished results.

(13) Mimoun, H.; Charpentier, R.; Mitscher, A.; Fischer, J.; Weiss, R. *J. Am. Chem. Soc.* **1980**, *102*, 1047.

(14) Tuck, D. G. *Comprehensive Organometallic Chemistry*; Wilkinson, G., Stone, F. G. A., Abel, E. W., Eds.; Pergamon: Oxford, 1982; Vol. 1, Chapter 7.

Evidence for Formation of Gaseous Methyl Radicals in the Decomposition of Methoxide on Oxygen-Precovered Mo(110)

J. G. Serafin and C. M. Friend*

Department of Chemistry, Harvard University
Cambridge, Massachusetts 02138

Received May 22, 1989

Evidence of the unprecedented formation of gaseous methyl radicals from adsorbed methoxide is presented in this study. Previously, surface methoxide has been found to either form formaldehyde or decompose to CO and H_2. The observation of methyl radicals during decomposition of methanol on Mo(110) precovered with atomic oxygen is of significance to the study of the partial oxidation of methane over metal oxide catalysts, since the observed decomposition pathway of methanol is analogous to the reverse of methane oxidation. Methyl radicals, produced from methane reaction over metal oxide catalysts,[1,2] evolve into the gas phase to form C_2 products or react on the catalyst to produce surface methoxide ions. Methyl radical formation is attributed solely to the direct abstraction of H from methane whereas ad-

(1) Driscoll, D. J.; Martir, W.; Wang, J.-X.; Lunsford, J. H. *J. Am. Chem. Soc.* **1985**, *107*, 58.

(2) Liu, H.-F.; Liu, R.-S.; Liew, K. Y.; Johnson, R. E.; Lunsford, J. H. *J. Am. Chem. Soc.* **1984**, *106*, 4117.

0002-7863/89/1511-8967$01.50/0